Environmental Earth Sciences (2024) 83:467
https://doi.org/10.1007/s12665-024-11772-2

ORIGINAL ARTICLE

A prediction model of mining subsidence based on an unskewed continuous probability distribution over an infinite interval

Hejian Yin[1] · Guangli Guo[1] · Huaizhan Li[1] · Tiening Wang[1]

Received: 2 April 2024 / Accepted: 21 July 2024 / Published online: 5 August 2024

Abstract

Mining subsidence is a serious threat to the ecosystems of mining regions. Accurate prediction of mining subsidence is essential for a scientific assessment of mining-induced damage. This study proposed a prediction model of mining subsidence based on an unskewed continuous probability distribution over an infinite interval. This method is an extension of the commonly used subsidence prediction method, the probability integration method, employed by Chinese engineers. It has the same scope of application as the probability integration method. This method does not have a specific expression and encourages engineers to screen appropriate unskewed continuous probability distribution functions and incorporate them into this model to establish prediction equations. By not solely considering one prediction method developed based on a specific function, it avoids limiting the improvement of prediction accuracy. The reliability of this method was validated by comparing it with actual subsidence data from the mining area. The results indicate that this approach can further improve the accuracy of mining subsidence prediction compared to the probability integration method.

Keywords Mining subsidence · Probability distribution · Prediction model · Probability integration method

Introduction

Mining may create substantial surface subsiding, leading to landslides, collapse, and other disasters (Fernandez et al. 2020; Kwinta and Gradka 2020; Salmi et al. 2017; Tajdus et al. 2018). Therefore, mining subsiding is a serious threat to the ecosystems of mining regions. Many scholars believe that accurate prediction of mining subsidence is beneficial for providing safe and efficient guidance in underground coal mining and scientifically evaluating the mining-induced environmental damage (Liu et al. 2022; Qin et al. 2023; Wang et al. 2022; Wei et al. 2023; Xu et al. 2023).

Currently, there are many kinds of prediction methods for mining subsidence. (1) Scholars regard bedrock and alluvium as two different media. A predictive model for mining subsidence is established by combining two separate models: an overlying strata movement model developed based on mechanics principles, and an alluvium movement model developed based on stochastic media theory. (Guo et al. 2020; Ma et al. 2021; Qin et al. 2023; Wang et al. 2022; Yang and Luo 2021). (2) Simulation method. Academics constructed finite element or discrete element numerical models according to stratigraphic information. Then, a surface subsidence prediction can be implemented by simulating coal mining (Alam et al. 2022; Gong et al. 2022; Jirankova et al. 2020; Liu et al. 2022). (3) The third method uses neural networks, fuzzy mathematics, and other theories to forecast subsiding (Alaee et al. 2019; Kumar et al. 2022). (4) The fourth method is the profile function approach. This method obtains a specific mathematical function by fitting the surface subsidence curve of a mining area and then using this function to predict surface subsidence within the mining area (Haciosmanoglu 2004; Saeidi et al. 2022). One drawback of this method is its limitation in predicting two-dimensional subsidence profiles rather than the entire three-dimensional subsidence basin (Saeidi et al. 2022). (5) The fifth method is the influence function method (IFM). This approach relies on theoretical study or other ways to calculate the subsidence caused by mining

✉ Guangli Guo
guangliguo@cumt.edu.cn

Hejian Yin
Yin_hj@cumt.edu.cn

[1] School of Environment and Spatial Informatics, China University of Mining and Technology, Xuzhou 221116, Jiangsu, China

basic mining units (represented by influence functions). Then, the subsiding of a particular place is considered to be the summation of the subsidence caused by the mining of basic mining units, according to the superposition principle. (Kratzsch and Fleming 1983; Malinowska et al. 2020; Saeidi et al. 2022). Compared to other methods, IFM has numerous advantages. This approach offers high computational efficiency (Malinowska et al. 2020). The IFM allows for rapid prediction of surface subsidence at any point within the gob using computer programs (Deng et al. 2014). Furthermore, compared with the mechanics method, this method requires fewer model parameters, and acquiring these parameters is relatively straightforward. The predictive parameters of the IFM can be obtained by inverting surface movement observation data (Chi et al. 2021). Many mining areas in China have abundant surface movement observation data, which provides convenient conditions for obtaining predictive parameters of the IFM. Therefore, this study will employ the theory of influence functions to establish the prediction model.

In China, the probability integration method (PIM) is the most commonly used method for predicting mining subsidence (Wei et al. 2023). This method also is a specific application of the IFM. According to the definition of PIM (Deng et al. 2014), mining with infinitesimal mining thickness and width is defined as element extraction. The subsidence basin at the surface induced by the element extraction is called the element basin. The mathematical expression for the element basin is called the element subsidence function. The element subsidence function of PIM follows a normal distribution. Then, using the element subsidence function as the influence function, according to the superposition principle, the PIM can be built using mathematical derivation. In other words, PIM is a prediction model developed based on the normal distribution function. Although PIM is widely used, it does not achieve satisfactory prediction results in some mining areas, especially those with thick alluvium (Jiang et al. 2020, 2022; Wei et al. 2023).

Compared to thin alluvium mining areas, thick alluvium mining areas exhibit larger surface subsidence areas and smaller limit angles. At the edges of subsidence basins, predicted surface subsidence values from PIM are significantly lower than actual measured subsidence values (Jiang et al. 2020, 2022). This phenomenon is referred to as the long-tailed distribution characteristic of surface subsidence. However, PIM is a prediction method developed based on the assumption of a normal distribution, which does not exhibit a long-tailed distribution. As a result, the predictive accuracy of PIM is lower at the periphery of the subsidence basin (Wei et al. 2023). Therefore, some scholars have also developed subsidence prediction models based on other function models to improve the accuracy of subsidence prediction (Chi et al. 2021; Wang et al. 2013; Zhang et al. 2022).

The aforementioned research indicates that prediction models developed based on the assumption of a normal distribution may not be the optimal choice for certain mining areas. To enhance the accuracy of subsidence prediction, this study attempted to extend the PIM to a prediction model for mining subsidence based on an unskewed continuous probability distribution over an infinite interval. This subsidence prediction model is named CPM. CPM is an extension of PIM, sharing the same fundamental principles and application scope. CPM relates the probability distribution function to the subsidence prediction. Unlike other prediction methods, it does not have a specific function expression. Instead, engineers are allowed to screen some appropriate probability distribution functions to incorporate into this model and establish subsidence prediction equations. The objective of this study is to enhance the accuracy of subsidence prediction. By not solely considering one prediction method developed based on a specific function, it avoids limiting the improvement of prediction accuracy.

Methods

CPM

The element subsidence function of the PIM can be expressed by Eq. (1).

$$\begin{cases} w_{pime}(x) = 1/r \ \exp\left(-\pi x^2/r^2\right) \\ r = H_0/\tan\beta \end{cases} \tag{1}$$

where x indicates the position of a certain point on the ground (m), r indicates the main influence radius (m), and H_0 indicates the average mining depth (m); tanβ indicates the tangent of main influence angle, which is a parameter of PIM.

The relationship between this element subsidence function and the probability density function (PDF) f_N of normal distribution is shown in Eq. (2).

$$\begin{cases} f_N\left(x,\mu_n,\sigma_n\right) = 1/\sqrt{2\pi}\sigma_n \exp\left(-\left(x-\mu_n\right)^2/2\sigma_n^2\right) \sim N\left(\mu_n,\sigma_n^2\right) \\ w_{pime}(x) \sim N\left(0,\left(r/\sqrt{2\pi}\right)^2\right) \end{cases} \tag{2}$$

where μ_n indicates the location parameter of the normal distribution, and σ_n indicates the scale parameter.

When $\mu_n = 0, \sigma_n = r/\sqrt{2\pi}$, the PDF of the normal distribution is equivalent to the element subsidence function of PIM. The so-called "main influence radius r" is also essentially the scale parameter of a probability distribution. Therefore, the PIM has a close connection to the normal distribution. The normal distribution has the following

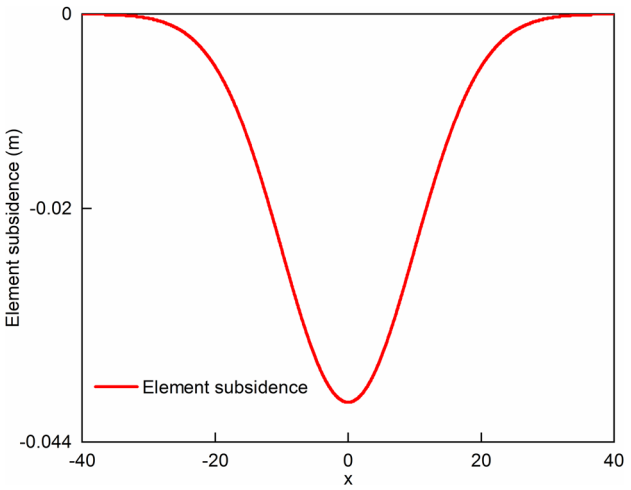

Fig. 1 Morphology of element subsidence function (take the PDF fN(x,0,10) of the normal distribution as an example)

two properties: (1) The independent variable is a single continuous random variable; (2) The interval of the independent variable is infinite. (3) The PDF presents an unskewed symmetrical distribution. We define this class of probability distributions as unskewed continuous probability distributions over an infinite interval. This section will extend the PIM to a prediction model of mining subsidence based on an unskewed continuous probability distribution over an infinite interval. This subsidence prediction model is named CPM.

PIM has two application conditions (Deng et al. 2014). (1) It is appropriate for forecasting ground subsiding with continuous distribution characteristics. (2) It can be used to predict the surface subsidence law with non-skewness characteristics. In mining areas with flat terrain, surface subsidence patterns of horizontal or gently inclined coal seam extraction generally present non-skewness characteristics. Thus, it is appropriate for forecasting ground subsiding induced by extracting horizontal coal or gently inclined seams (the dip angle is less than 15°).

The CPM proposed in this study is an extension of the PIM. Therefore, CPM has the same scope of application as PIM. The CPM is not a generalized model, and its applicability is limited. In addition, the fundamental principles of PIM and CPM are influence function theory. The basic principles of this theory are as follows (Deng et al. 2014; Guo and Chai 2013).

The IFM divides the panel into multiple infinitesimally small mining units and calculates the impact of each unit's mining on surface subsidence. This impact is typically expressed using a function called the influence function. The influence function used in the CPM is an unskewed continuous probability distribution over an infinite interval. The surface subsidence caused by large-scale underground mining can be considered as the linear superposition of subsidence caused by all the small mining units. This superposition process can be seen as an integration process in probability theory. Therefore, the theoretical foundation of the IFM is based on the principle of linear superposition.

An element subsidence function

According to the definition of the unskewed continuous probability distribution over an infinite interval, its PDF $f(x, \mu, \sigma)$ and its cumulative distribution function (CDF) $F(x, \mu, \sigma)$ have the following properties.

$$\begin{cases} f \geq 0 \\ \int_{-\infty}^{+\infty} f(x,\mu,\sigma)dx = 1 \\ \begin{cases} F(x,\mu,\sigma) = \int_{-\infty}^{x} f(t,\mu,\sigma)dt \\ F(\mu,\mu,\sigma) = 0.5 \end{cases} \end{cases} \tag{3}$$

When $\mu = 0$, $f(x, 0, \sigma)$ is the element subsidence function of CPM. In Eq. (3), σ is defined as the main influence radius. The connection between the PIM's main influence radius r and the CPM's main influence radius σ is: $r/\sigma = \sqrt{2\pi}$. σ is calculated according to the following formula.

$$\sigma = H_0 / \tan\gamma \tag{4}$$

where $\tan\gamma$ indicates the tangent of main influence angle, which is a parameter of CPM.

Although there are various element subsidence functions, the curve shape of element subsidence functions generally presents the distribution characteristics of low at both ends and high at the middle (see Fig. 1), called a bell curve. Therefore, when screening the element subsidence function, engineers should screen the PDF whose morphological characteristic is a bell curve. Furthermore, this paper only discusses the forecasting model for mining subsidence developed based on an unskewed continuous probability distribution over an infinite interval. Thus, the PDF chosen by the researchers must present an unskewed symmetric distribution (see Fig. 1).

A prediction equation of subsidence on a major section for semi-infinite extraction of horizontal coal seams

In a surface subsidence basin, the vertical section along the strike or dip of the coal seam through the maximum subsidence point on the surface is called the major section. The horizontal coal seam's extraction depth is H_0 (see Fig. 2). When the horizontal coal seam on one side of the open-off cut has not been extracted, and the coal seam in other directions has been fully extracted, this mining condition is named as semi-infinite mining of horizontal coal seam. This section will derive a prediction equation of subsidence on the major section for the semi-infinite extraction of horizontal coal seams. The derivation process is similar to that of PIM. First, the coordinate system for the surface needed to be established (see Fig. 2). Point O above the boundary of the working face is used as the origin of the x-axis. The x-axis points toward the gob. $W(x)$ is the vertical axis, expressed as a given point's subsidence. In addition, a coordinate system for the coal seam needed to be established (see Fig. 2). The O_1 of the coal seam roof is the origin of the s-axis. The s-axis points to the gob. Both axes have the same scale. The maximum sinking w_0 is not equal to the mining height m due to the swellability of broken rock—$w_0 = mq$, where q indicates the subsidence factor, which is a CPM parameter. Thus, the mining height can be considered as mq. Referring to the derivation process of the PIM (Deng et al. 2014), the derivation process of the prediction equation of subsidence on a major section for semi-infinite extraction of horizontal coal seams was as follows.

As shown in Fig. 2, the coordinate of any point A on the surface is x, and the abscissa of the extraction element is s. The sinking value on point A induced by the element extraction is given by:

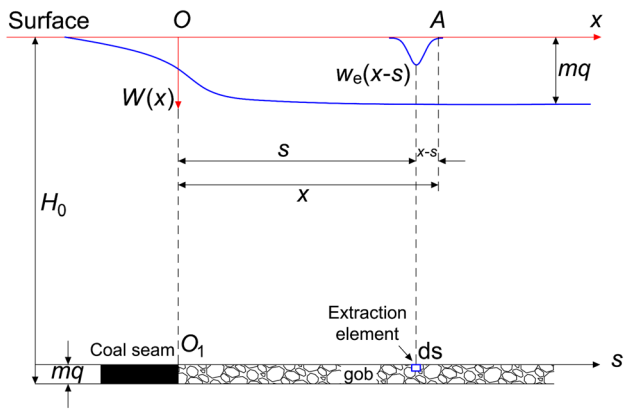

Fig. 2 Subsidence on the major section for semi-infinite extraction of horizontal coal seams

$$w_e(x-s) = f\left(x-s, 0,\ H_0/\tan\gamma\right) \tag{5}$$

The sum of point A subsiding caused by the mining of each element in the range of $s = 0 \sim +\infty$ was given by:

$$W(x) = \int_0^{+\infty} mqf\left(x-s, 0, H_0/\tan\gamma\right)ds \tag{6}$$

Set $x - s = t$. When $s = 0$, $t = x$; when $s = +\infty$, $t = -\infty$; d$(x\text{-}s) = -$dt, therefore:

$$\begin{aligned} W(x) &= -mq\int_x^{-\infty} f\left(t, 0, H_0/\tan\gamma\right)dt \\ &= mq\int_{-\infty}^{x} f\left(t, 0, H_0/\tan\gamma\right)dt \end{aligned} \tag{7}$$

From Eq. (3), we can get the following.

$$W(x) = mq\int_{-\infty}^{x} f\left(t, 0, H_0/\tan\gamma\right)dt = mqF\left(x, 0, H_0/\tan\gamma\right) \tag{8}$$

Equation (8) is the prediction equation of subsidence on a major section for semi-infinite extraction of horizontal coal seams. This equation is expressed as the product of the maximum subsidence value mq and the CDF $F(\bullet)$.

A prediction equation of subsidence on a major section for finite extraction of gently inclined seams

As shown in Fig. 3 (a) and (b), when all coal along the strike (or the dip of the coal seam) has been extracted, but the mining degree along the dip (or along the strike) is still subcritical mining, this mining condition is defined as finite extraction of the coal seam.

Before deriving the relevant equations, the term "the inflection point" was introduced. It is the cut-off point of the concave-convex change on the sinking curve, i.e., the point where the curvature is 0 (Deng et al. 2014). According to Eqs. (3) and (8), if the element subsidence function of a mining area follows an unskewed symmetrical distribution, the inflection point of the subsidence curve on a major section for semi-infinite extraction of horizontal coal seams will be located directly above the gob boundary. In fact, the inflection point will be offset to the left or right along the direction of the coal seam, influenced by the cantilever roof or the adjacent gob. Define this offset distance as the deviation of inflection point, which is the

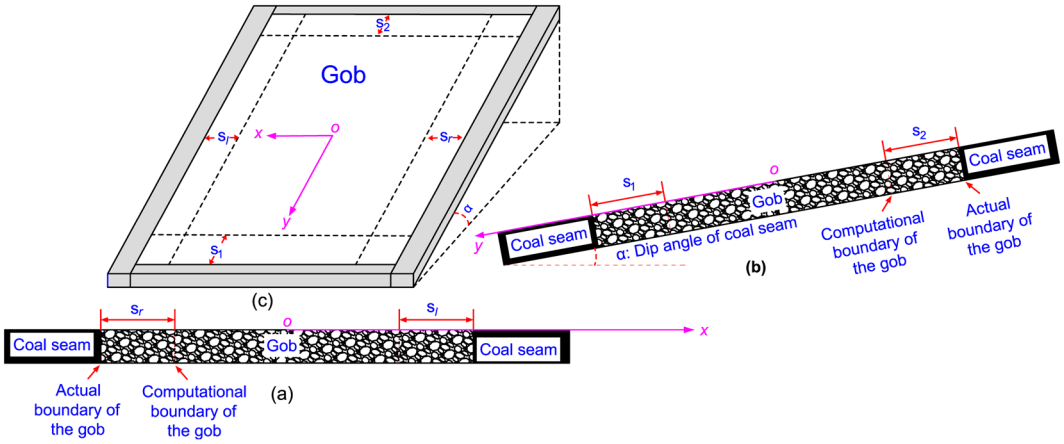

Fig. 3 Definition of finite extraction: **a** Finite extraction along the strike of the coal seam, **b** Finite extraction along the dip of the coal seam, **c** Distribution positions of four kinds of deviations of inflection point

parameter of the CPM. When calculating ground subsidence, the offsetting of the gob boundary can be used to achieve the offsetting of the inflection point, referring to the derivation process for PIM. Thus, the deviation of inflection point can be regarded as the distance that the gob's computational boundary deviates from the real boundary (see Fig. 3 (a) and (b)). If this parameter is positive, it means that the computational boundary is on one side of the gob. At this point, the computational length of the gob will be shortened. If this parameter takes a negative value, the computational boundary is on the coal pillar's side. At this point, the gob's computational length will be enlarged. If this parameter is 0, the computational boundary of the gob coincides with the actual boundary of the gob. The deviation of inflection point is generically positive or zero if no other gobs are around the gob. Otherwise, it is negative. As shown in Fig. 3 (c), according to the different positions, the deviation of inflection point is divided into the deviation of inflection point along the dip side of the coal seam (s_1), the deviation of inflection point along the rising side of the coal seam (s_2), the deviation of inflection point along the left side (s_l), and the deviation of inflection point along the right side (s_r). If the coal seam is horizontal, the inflection point after offset will be directly above the gob boundary after offset (computational boundary of gob).

This section will first derive a prediction equation for subsidence on a major section along the dip of a coal seam in the case of a finite extraction of a gently inclined seam.

As shown in Fig. 4 (a), A and B are the actual boundaries of the gob, and C_1 and D_1 are the computational boundaries of the gob. s_1 and s_2 are the deviations of inflection point

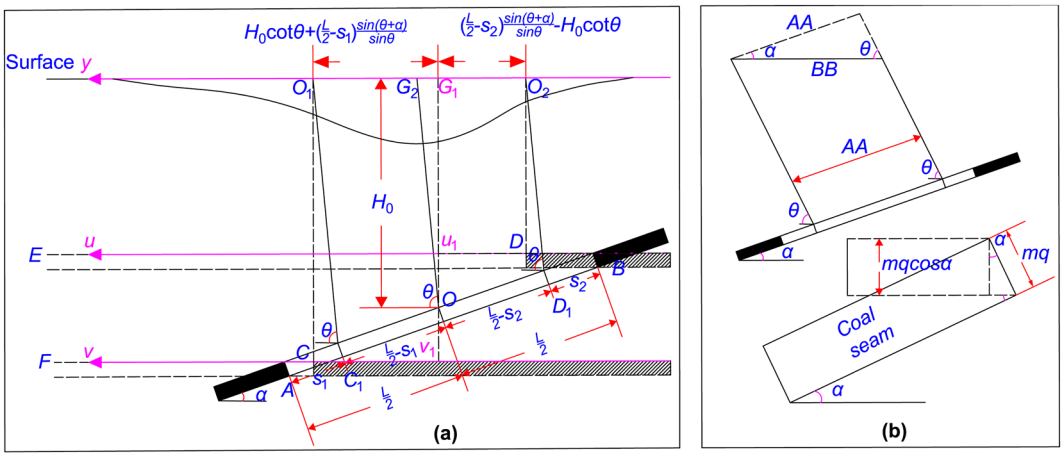

Fig. 4 Computational principles of subsidence on a major section along the dip of the coal seam for finite extraction of gently inclined seams: **a** Create a coordinate system, **b** Relationship between length and height along gently inclined seams and length and height along horizontal coal seams

along the dip and rising sides of the coal seam, respectively. When the coal seam and overlying strata are inclined, mining influence spreads at an angle to the surface rather than vertically upward. Due to the inclination of the coal seam and overlying strata, the inflection point will not be located directly above the computational boundary of the gob, but will be offset toward the dip direction of the coal seam (Deng et al. 2014). The inflection points after the offset are located at O_1 and O_2, respectively. In addition, the maximum subsidence point is not located at G_1 directly above the center O of the gob, and will be offset toward the dip of the coal seam (see Fig. 4 (a)). G_2 is the maximum sinking point after the offset. As shown in Fig. 4 (a), the angle on one side of the dip direction of the coal seam between the line connecting the inflection point after offset and the calculation boundary on the same side and the horizontal line is defined as the influence transference angle θ. θ is a parameter of the CPM. The length of G_1G_2 is $H_0\cot\theta$.

According to the calculation principle of the PIM (Deng et al. 2014), the calculation of surface subsidence induced by finite extraction of gently inclined seams is essentially the difference between the surface subsidence induced by semi-infinite extraction of two horizontal coal seams. As seen in Fig. 4 (a), the surface subsidence caused by finite extraction with the computational boundary C_1D_1 (equivalent to the actual boundary AB) is equal to the difference between the ground subsiding induced by semi-infinite extraction of horizontal coal seams DE and CF.

As shown in Fig. 4 (b), after a gently inclined seam is naturalized into a horizontal coal seam, the mining height of the coal seam is $mq\cos\alpha$. As seen in Fig. 4 (b), according to the law of sine, the relationship between the length AA along the inclination direction of the coal seam and the length BB along the horizontal direction is:

$$AA/\sin\theta = BB/\sin(180-\alpha-\theta) = BB/\sin(\alpha+\theta) \tag{9}$$

Thus:

$$BB = AA\sin(\alpha+\theta)/\sin\theta \tag{10}$$

According to Eq. (10), the gob length L, s_1, and s_2 along the horizontal direction are $L\sin(\alpha+\theta)/\sin\theta$, $s_1\sin(\alpha+\theta)/\sin\theta$ and $s_2\sin(\alpha+\theta)/\sin\theta$.

As shown in Fig. 4 (a), a surface coordinate system was established. Taking the G_1 point just above the center of the gob as the origin, the y-axis points to the left (the y-axis generally points toward the dip direction). The coordinate system's origins for two horizontal coal seams are u_1 and v_1, respectively. They lie on the same vertical line as the surface coordinate system's origin. In addition, the coordinate systems u and v of the coal seams have the same orientation and scale as the surface coordinate system. The extraction range of horizontal coal seam DE is $u\in((-L/2+s_2)\sin(\alpha+\theta)/\sin\theta+H_0\cot\theta,+\infty)$. The extraction range of horizontal coal seam CF is $v\in((L/2-s_1)\sin(\alpha+\theta)/\sin\theta+H_0\cot\theta,+\infty)$.

The ground sinking $W^0_{(y)}$ induced by finite extraction with the computational boundary C_1D_1 is equal to the difference between the surface subsidence induced by semi-infinite extraction for horizontal coal seams DE and CF; the relevant equations were derived as follows:

$$\begin{aligned} W^0_{(y)} = &\int_{H_0\cot\theta+\left(-L/2-s_1\right)\sin(\alpha+\theta)/\sin\theta}^{+\infty} mq\cos\alpha f\left((y-u),0,\ H_0/\tan\gamma\right)du \\ &-\int_{H_0\cot\theta+\left(L/2-s_1\right)\sin(\alpha+\theta)/\sin\theta}^{+\infty} mq\cos\alpha f\left((y-v),0,\ H_0/\tan\gamma\right)dv \end{aligned} \tag{11}$$

Set $y-u=t$. When $u=+\infty$, $t=-\infty$; when $u=H_0\cot\theta+(-L/2+s_2)\sin(\alpha+\theta)/\sin\theta$, $t=y-H_0\cot\theta+(L/2-s_2)\sin(\alpha+\theta)/\sin\theta$; $\mathrm{d}(y-u)=-\mathrm{d}t$. Set $y-v=t$. When $v=+\infty$, $t=-\infty$; when $v=H_0\cot\theta+(L/2-s_1)\sin(\alpha+\theta)/\sin\theta$, $t=y-H_0\cot\theta-(L/2-s_1)\sin(\alpha+\theta)/\sin\theta$; $\mathrm{d}(y-v)=-\mathrm{d}t$. Substitute them into the upper and lower limits of the integral to obtain the following:

$$\begin{aligned} W^0_{(y)} = &mq\cos\alpha\left(-\int_{y-H_0\cot\theta+(L/2-s_2)\sin(\alpha+\theta)/\sin\theta}^{-\infty} f\left(t,0,\ H_0/\tan\gamma\right)dt\right)+ \\ &mq\cos\alpha\left(\int_{y-H_0\cot\theta-(L/2-s_1)\sin(\alpha+\theta)/\sin\theta}^{-\infty} f\left(t,0,\ H_0/\tan\gamma\right)dt\right) \end{aligned} \tag{12}$$

After transforming the upper and lower bounds of the integral, we can obtain the following.

$$\begin{aligned} W^0_{(y)} = &mq\cos\alpha\left(\int_{-\infty}^{y-H_0\cot\theta+(L/2-s_2)\sin(\alpha+\theta)/\sin\theta} f\left(t,0,\ H_0/\tan\gamma\right)dt\right)- \\ &mq\cos\alpha\left(\int_{-\infty}^{y-H_0\cot\theta-(L/2-s_1)\sin(\alpha+\theta)/\sin\theta} f\left(t,0,\ H_0/\tan\gamma\right)dt\right) \end{aligned} \tag{13}$$

Having solved the definite integral, we can obtain the following result.

$$\begin{aligned} W^0_{(y)} = &mq\cos\alpha F\left(y-H_0\cot\theta+(L/2-s_2)\sin(\alpha+\theta)/\sin\theta,0,\ H_0/\tan\gamma\right) \\ &-mq\cos\alpha F\left(y-H_0\cot\theta-(L/2-s_1)\sin(\alpha+\theta)/\sin\theta,0,\ H_0/\tan\gamma\right) \end{aligned} \tag{14}$$

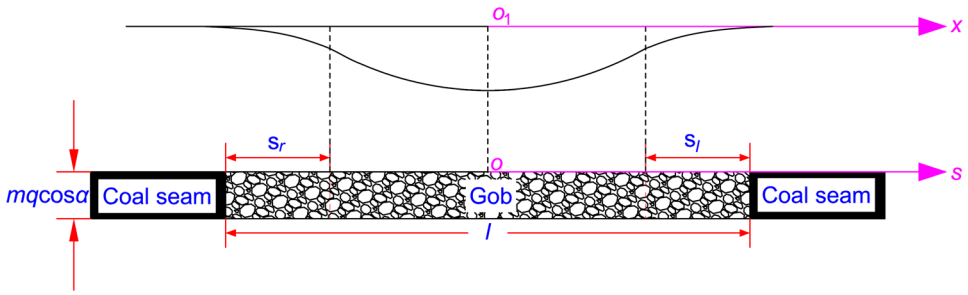

Fig. 5 Computational principles of subsidence on a major section along a strike of a coal seam in the case of a finite extraction of a gently inclined seam

Equation (14) is the prediction equation for subsidence on a major section along the dip of the coal seam in the case of finite extraction of gently inclined seams.

This section will then derive the prediction equations for subsidence on a major section along the strike of a coal seam in the case of a finite extraction of a gently inclined seam.

First, a coordinate system was established for the surface. The origin O_1 of the x-axis coordinate is located just above the center of the gob, and the x-axis points to the right (see Fig. 5). The mining length along the strike of the coal seam is l. s_l and s_r are the deviations of inflection points along the left and right sides of the coal seam, respectively. The origin of the coal seam coordinate system's s-axis, O, is set in the middle of the gob and points to the right. In addition, the coordinate system for the coal seam has the same orientation and scale as the coordinate system for the surface. Therefore, when the excavation range is $s \in (-0.5\ l+s_r, 0.5\ l\text{-}s_l)$, the sinking at a point x on the ground is given by:

$$W_{(x)}^0 = mq\cos\alpha \int_{-0.5l+s_r}^{0.5l-s_l} f\left(x-, 0, H_0/\tan\gamma\right)ds \tag{15}$$

Set x - $s = t$. When $s = -0.5\ l+s_r$, $t = x+0.5\ l\text{-}s_r$; when $s = 0.5\ l\text{-}s_l$, $t = x\text{-}(0.5\ l\text{-}s_l)$; d($x$-$s$) = − d$t$. Thus:

$$\begin{aligned} W_{(x)}^0 &= mq\cos\alpha \int_{x+0.5l-s_r}^{x-(0.5l-s_l)} -f\left(t, 0, H_0/\tan\gamma\right)dt \\ &= mq\cos\alpha \int_{x-(0.5l-s_l)}^{x+0.5l-s_r} f\left(t, 0, H_0/\tan\gamma\right)dt \end{aligned} \tag{16}$$

Having solved the definite integral, we can obtain the following result.

$$\begin{aligned} W_{(x)}^0 = mq\cos\alpha\big(&F\left(\left(x+0.5l-s_r\right), 0, H_0/\tan\gamma\right) \\ &-F\left(\left(x-0.5l+s_l\right), 0, H_0/\tan\gamma\right)\big) \end{aligned} \tag{17}$$

Equation (17) is the prediction equation for subsidence on a major section along the strike of the coal seam in the case of finite extraction of gently inclined seams. It is also essentially the difference between the surface subsidence induced by the semi-infinite extraction of two coal seams.

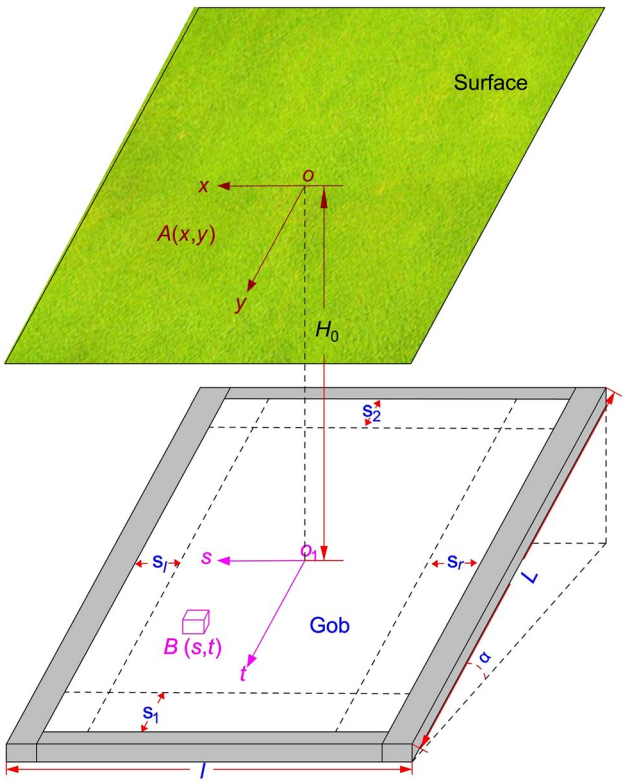

Fig. 6 Coordinate system for the surface and coal seam

A prediction equation of subsidence at any point on the surface induced by the extraction of a rectangular panel

First, a coordinate system was established for the surface and coal seams. As illustrated in Fig. 6, the origin of the coal seam's coordinate system, sO_1t lies in the gob's center, with the t-axis pointing towards the coal seam's dip. The horizontal projection of the coordinate system sO_1t for the coal seam coincides with that of the coordinate

system xOy for the surface. Under two-dimensional conditions, the forecasting formula for ground subsidence induced by element extraction is shown in Eq. (5). Under three-dimensional conditions, the ground sinking is influenced by the combined influence of extraction along the coal seam's strike and dip (Deng et al. 2014). According to the influence function theory, the subsiding for point A (coordinates (x, y)) on the ground induced by the extraction of element B (coordinates (s, t)) is the following.

$$w_e(x,y) = f\left(x-s,0,H_0/\tan\gamma\right)f\left(y-t,0,H_0/\tan\gamma\right) \quad (18)$$

The mining length along the strike is l. The mining length along the dip is L, as illustrated in Fig. 6. The extraction range along the strike is $s\in(-0.5\,l+s_r,0.5\,l-s_l)$ (see Fig. 6). Due to the inclination of the coal seam, the mining length and height along the dip of the coal seam needs to be converted to the mining length and height along the horizontal coal seam. Therefore, the mining height of the coal seam is $mq\cos\alpha$. The extraction range along the coal seam's dip is $t\in((-L/2+s_2)\sin(\alpha+\theta)/\sin\theta+H_0\cot\theta,\ (L/2-s_1)\sin(\alpha+\theta)/\sin\theta+H_0\cot\theta)$. The sinking at point A on the ground induced by the extraction of a rectangular panel is as follows.

$$\begin{aligned} w(x,y) = &\int_{-0.5l+s_r}^{0.5l-s_l} \\ &\int_{H_0\cot\theta+(-L/2+s_2)\sin(\alpha+\theta)/\sin\theta}^{H_0\cot\theta+(L/2-s_1)\sin(\alpha+\theta)/\sin\theta} mq\cos\alpha f\left(x-s,0,H_0/\tan\gamma\right) \\ &\times f\left(y-t,0,H_0/\tan\gamma\right)dtds \end{aligned} \quad (19)$$

$$\begin{aligned} w(x,y) = &mq\cos\alpha\int_{-0.5l+s_r}^{0.5l-s_l} f\left(x-s,0,H_0/\tan\gamma\right)ds \\ &\times\int_{H_0\cot\theta+(-L/2+s_2)\sin(\alpha+\theta)/\sin\theta}^{H_0\cot\theta+(-L/2-s_1)\sin(\alpha+\theta)/\sin\theta} \\ &f\left(y-t,0,H_0/\tan\gamma\right)dt \end{aligned} \quad (20)$$

Equation (21) can be obtained based on the derivation process of Eq. (14) and (17).

$$\begin{aligned} w(x,y) &= mq\cos\alpha\begin{pmatrix} F\left(x+0.5l-s_r,0,H_0/\tan\gamma\right) \\ -F\left(x-0.5l+s_l,0,H_0/\tan\gamma\right)\end{pmatrix} \\ &\times\begin{pmatrix} F\left(y-H_0\cot\theta+\left(L/2-s_1\right)\sin(\alpha+\theta)/\sin\theta,0,H_0/\tan\gamma\right) \\ -F\left(y-H_0\cot\theta-\left(L/2-s_1\right)\sin(\alpha+\theta)/\sin\theta\ ,0,H_0/\tan\gamma\right)\end{pmatrix} \\ &= W^0_{(x)}W^0_{(y)}/mq\cos\alpha \end{aligned} \quad (21)$$

Equation (21) is the prediction equation of subsidence at any point on the surface induced by the extraction of a rectangular panel. In other words, Eq. (21) is the prediction model for mining subsidence at any point on the surface based on an unskewed continuous probability distribution over an infinite interval. This equation is a forecasting formula for the ground subsidence induced by the extraction of the rectangular panel. This prediction model has at least seven parameters. They are, respectively, the tangent of main influence angle ($\tan\gamma$), the subsidence factor (q), the influence transference angle (θ), the deviation of inflection point along the dip side of the coal seam (s_1), the deviation of inflection point along the rising side of the coal seam (s_2), the deviation of inflection point along the left side (s_l), and the deviation of inflection point along the right side (s_r).

Application method of CPM

The scope of application for the CPM is identical to that of PIM. It is suitable for predicting the continuous and non-skewed subsidence patterns caused by exploiting horizontal or gently inclined coal seams. Therefore, engineers need to determine whether the subsidence pattern in a mining area aligns with the applicability of the CPM. The proposed CPM in this paper is a prediction model that does not have specific expressions, making it unsuitable for directly predicting surface subsidence. First, engineers should select specific probability distribution functions. Second, these distribution functions can be incorporated into the CPM to transform the CPM into a subsidence prediction model based on the specific distribution function. Finally, the prediction of surface subsidence in mining areas can be achieved using the subsidence prediction model based on the specific distribution function.

The chosen probability distribution function needs to satisfy two criteria. First, the selected probability distribution function must be based on an unskewed continuous probability distribution over an infinite interval. Second, the accuracy with which the selected probability distribution function is fitted to the surface subsidence curve needs to meet the corresponding requirements. In practical engineering, the root-mean-square error $RMSE$ (mm) and the relative error RE (%) are generally used to evaluate the fitting accuracy. Their calculation methods are shown in Eqs. (22) and (23), respectively.

$$RMSE = \sqrt{\sum_{i=1}^{N}\left(w_{im}-w_{ip}\right)^2/N} \quad (22)$$

$$RE = RMSE/W_{\max} \quad (23)$$

where N represents the total number of observation points. w_{im} and w_{ip} indicate the measured and predicted values of an observation point i, respectively (mm). $W_{\max}$ is the maximum subsidence value (mm).

Relationship with the PIM

The following is the normal distribution's CDF:

$$F_N = {}^1/_2\left(1 + erf\left(x - u_n/\sigma_n\sqrt{2}\right)\right) \tag{24}$$

Set $\sigma = \sigma_n = {}^r/\sqrt{2\pi}$, r indicates the main influence radius for the PIM. $r = H_0/\tan\beta$. $\tan\beta$ indicates the tangent of main influence angle for the PIM. The relationship between $\tan\beta$ and $\tan\gamma$ is as follows.

$$\tan\gamma = H_0/\sigma = H_0/\left(r/\sqrt{2\pi}\right) = \sqrt{2\pi}\left(H_0/r\right) = \sqrt{2\pi}\tan\beta \tag{25}$$

Replace CDF $F(\bullet)$ in Eq. (21) with the CDF F_N of normal distribution. Set $\mu_n = 0$, $\tan\gamma = \sqrt{2\pi}\tan\beta$, can be obtained:

$$W_{pim}(x,y) = mq\cos\alpha\left[W_{PIM}\left(x + 0.5l - s_r\right) - W_{PIM}\left(x - 0.5l + s_l\right)\right] \times \left[\begin{array}{c} W_{PIM}\left(y - H_0\cot\theta + \left({}^{L}/_{2-s_1}\right)^{\sin(\alpha+\theta)}/\sin\theta\right) \\ -W_{PIM}\left(\sin\theta - \left({}^{L}/_{2-s_1}\right)^{\sin(\alpha+\theta)}/\sin\theta\right) \end{array}\right] \tag{26}$$

$$W_{PIM}(X) = \frac{1}{2}\left(1 + erf\left(\frac{\tan\beta X\sqrt{\pi}}{H_0}\right)\right) \tag{27}$$

Equation (27) is the prediction equation for sinking at any point on the ground based on the PIM. It is a special case of the CPM.

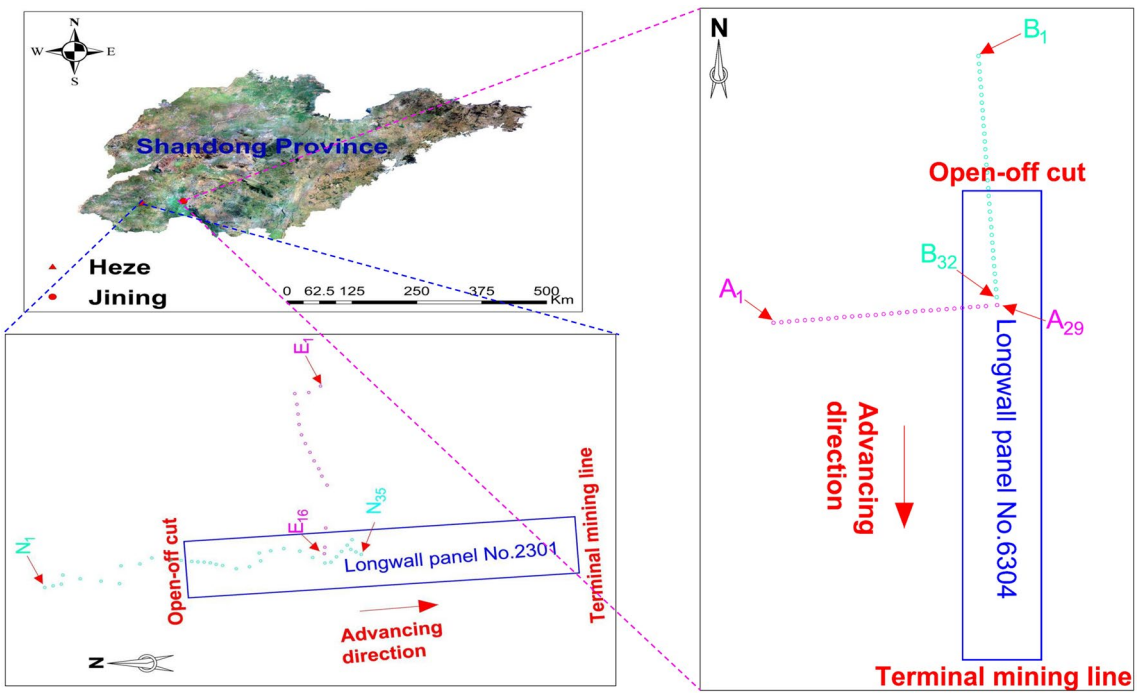

Fig. 7 Geographic location of the study area and relative positions of the longwall panel and observation line

Table 1 The geological and mining conditions

Panel	Width (m)	Length (m)	Average mining depth (m)	Mining height (m)	Dip angle of the coal seam (°)	Thickness of alluvium (m)
No.6304	250	1503	700	4.4	2.0	199
No.2301	261	1635	862	8.5	5.8	160

Method validation

As shown in Fig. 7, taking two coal mines in Jining and Heze cities, Shandong province, China, as examples, these mines have previously extracted panels numbered 6304 and 2301, respectively. The roof management method employed is caving. The geological and mining conditions of the two panels are shown in Table 1. Two observation lines were set up above each panel to study the subsidence mining law (see Fig. 7). These lines include one along the strike direction of the panel and another along the dip direction. The terrain above the gob is relatively flat. Engineers utilized leveling measurements to monitor surface subsidence when it ceased. Both mining areas exhibit a continuous distribution pattern of surface subsidence. Table 1 shows that both mining areas extracted gently inclined seams, fulfilling the conditions for using the CPM model to predict surface subsidence in these mining areas. Decision-makers have requested that the engineer select appropriate distribution functions to incorporate into the CPM model to establish a suitable surface subsidence prediction model for these two mining areas.

According to Table 1, it can be observed that both mining areas have thick alluvium. Based on experience, subsidence in mining areas with thick alluvium exhibits a long-tailed distribution characteristic. Therefore, probability distributions with long-tailed characteristics should be selected. In this study, the Logistic distribution, T Location-Scale distribution, Laplace distribution, and Cauchy distribution were chosen to construct subsidence prediction models and fit the subsidence data (Fang and Xu 2016; Li 2016; Yin et al. 2022).

The main influence radius r of the PIM and the main influence radius σ_f of the CPM are both scale parameters of probability distributions. Their relationship is given by $\sigma_f = {}^{r}\Big/\sqrt{2\pi}$. To ensure numerical proximity between the main influence radius σ_f of various subsidence prediction models and the main influence radius r of the PIM, let the location parameter and scale parameter for these distribution functions be set as $\mu_f = 0, \sigma_f = {}^{r}\Big/\sqrt{2\pi}$, respectively. All subsidence prediction models used r as the main influence radius. The transformed PDFs and CDFs for each distribution function are shown in Table 2.

In Table 2, $\Gamma(\bullet)$ denotes the gamma function, and ${}_2F_1(\bullet)$ represents the Gaussian hypergeometric function. In the T Location-Scale distribution, the parameter ν represents the degree of freedom. A smaller value of ν indicates a longer tail in the distribution (Yin et al. 2022).

Then, substitute the CDFs from Table 2 into Eq. (21) to establish the subsidence prediction models based on the Logistic distribution, Cauchy distribution, T Location-Scale distribution, and Laplace distribution. These subsidence prediction models are named LOM, CM, TM, and LAM, respectively. The LOM is equivalent to the subsidence prediction model based on the Boltzmann function (Wang et al. 2013). The observed subsidence data of mining areas in Jining and Heze were fitted using these prediction models. The particle swarm optimization algorithm was used to match these prediction models with observed surface subsidence data. A comparison was made between the predictive accuracy of these forecasting models and that of the commonly used PIM among Chinese engineers. The fitting results for the two mining areas are shown in Fig. 8 and Fig. 9, while the fitting accuracy is presented in Table 3 and Table 4.

Table 3 and Table 4: In both tables, "m_t" refers to the overall fitting accuracy of the subsidence basin, while "m_e" represents the fitting accuracy of the subsidence data outside the gob (i.e., at the outer edge of the basin). This accuracy is

Table 2 Transformed PDF and CDF

Probability distribution	PDF(Element subsidence function) $f\left(x, 0, \frac{r}{\sqrt{2\pi}}\right) =$	CDF $F\left(x, 0, \frac{r}{\sqrt{2\pi}}\right) =$
Logistic distribution	$\frac{\sqrt{2\pi}}{r}\frac{\exp\left(\frac{-x\sqrt{2\pi}}{r}\right)}{\left(1+\exp\left(\frac{-x\sqrt{2\pi}}{r}\right)\right)^2}$	$\frac{1}{1+\exp\left(-\frac{x\sqrt{2\pi}}{r}\right)}$
Cauchy distribution	$\frac{\sqrt{2\pi}}{\pi r\left[1+\left(\frac{x\sqrt{2\pi}}{r}\right)^2\right]}$	$\frac{1}{\pi}\arctan\left(\frac{x\sqrt{2\pi}}{r}\right)+\frac{1}{2}$
T Location- Scale distribution	$\frac{\sqrt{2}\Gamma\left(\frac{\nu+1}{2}\right)}{r\Gamma\left(\frac{\nu}{2}\right)\sqrt{\nu}}\left(1+\frac{2\pi x^2}{\nu r^2}\right)^{-\frac{\nu+1}{2}}$	$\frac{1}{2}+\frac{\sqrt{2}x\Gamma\left(\frac{\nu+1}{2}\right){}_2F_1\left(\frac{1}{2},\frac{\nu+1}{2};\frac{3}{2};-\frac{2\pi x^2}{\nu r^2}\right)}{r\Gamma\left(\frac{\nu}{2}\right)\sqrt{\nu}}$
Laplace distribution	$\left(\frac{\sqrt{2\pi}}{2r}\right)\exp\left(\frac{-\sqrt{2\pi}\lvert x\rvert}{r}\right)$	$\begin{cases} 0.5\exp\left(x\sqrt{2\pi}\Big/r\right), x<0 \\ 1-0.5\exp\left(-x\sqrt{2\pi}\Big/r\right), x\geq 0 \end{cases}$

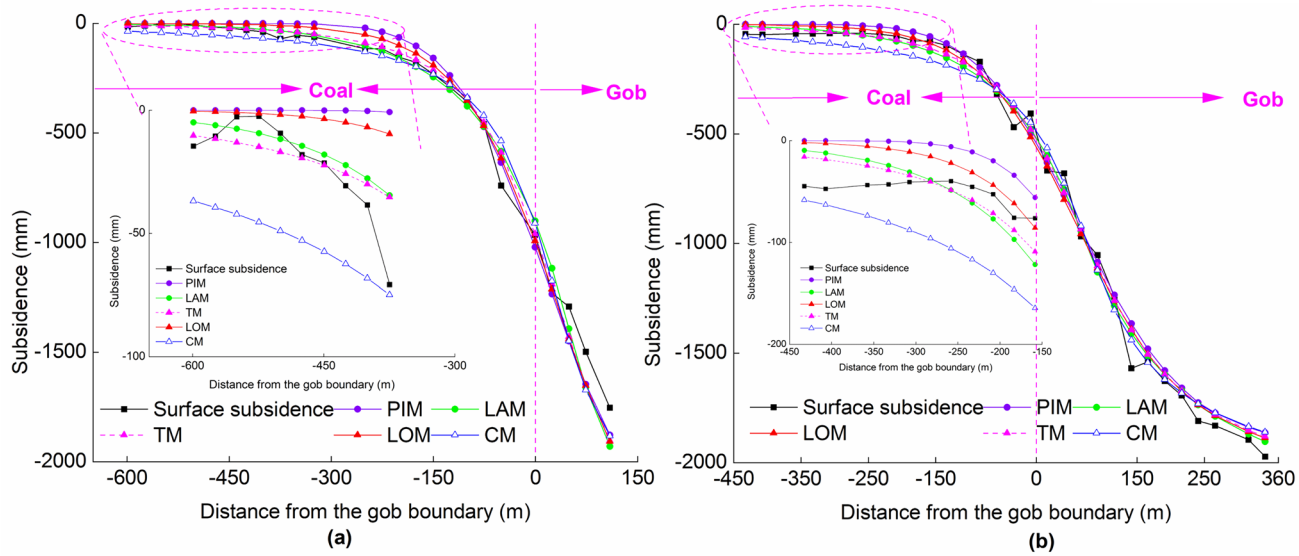

Fig. 8 Fitting performance of subsidence in the Jining mining area: **a** Line A, **b** Line B

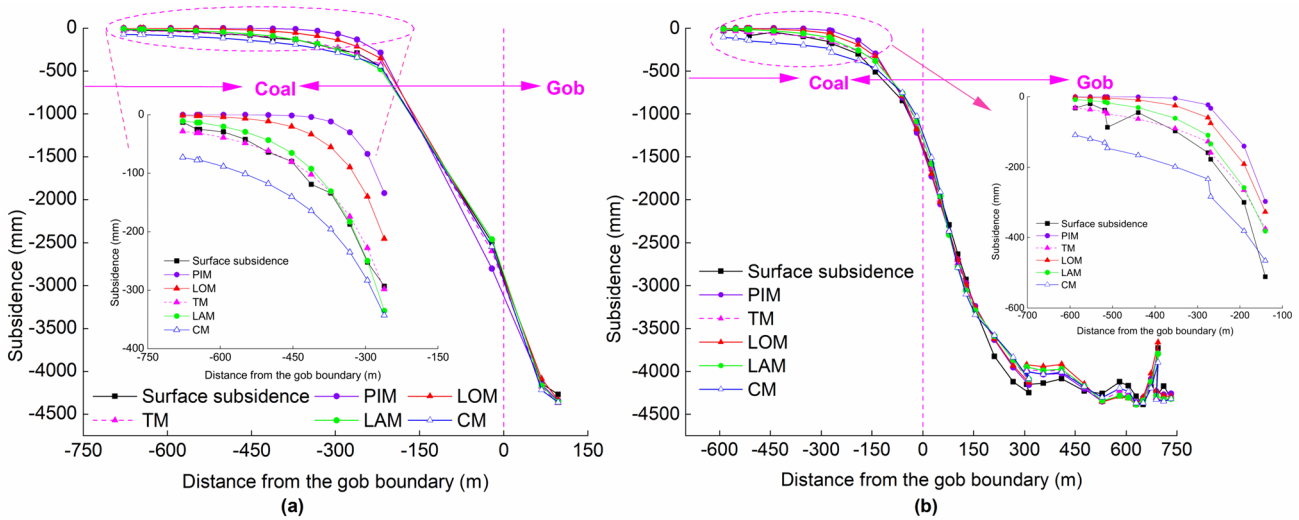

Fig. 9 Fitting performance of subsidence in the Heze mining area: **a** Line E, **b** Line N

Table 3 Parameters and accuracies of the model obtained from the fit (Jining mining area)

Model	q	tanγ	θ (°)	ν	s_l (m)	s_r (m)	s_1 (m)	s_2 (m)	m_t (mm)	m_e (mm)
PIM	0.608	2.371	90	/	− 70	33	56	0	67.0	51.2
LOM	0.669	3.798	90	/	− 70	43	55	0	61.1	42.1
CM	0.744	3.568	90	/	− 70	28	70	70	69.7	58.0
TM	0.696	2.747	90	2.64	− 56	40	62	16	57.7	36.7
LAM	0.730	2.441	90	/	− 70	50	63	70	60.3	40.4

used to describe the fitting performance of the model at the peripheral locations of the subsidence basin.

According to Table 3, all models have a relative error of less than 4% in fitting in the Jining mining area. The ranking of overall fitting accuracy for the entire

Table 4 Parameters and accuracies of the model obtained from the fit (Heze mining area)

Model	q	tanγ	θ (°)	ν	s_l (m)	s_r (m)	s_1 (m)	s_2 (m)	m_t (mm)	m_e (mm)
PIM	1.333	2.548	88	/	29	60	78	53	109.6	120.7
LOM	1.254	4.207	89	/	65	62	62	62	100.7	75.9
CM	0.898	4.161	87	/	100	72	37	0	103.2	77.1
TM	0.906	3.214	87	2.32	55	66	54	10	85.2	44.6
LAM	0.855	2.887	87	/	72	65	53	0	93.0	46.8

subsidence basin, from highest to lowest, is as follows: TM > LAM > LOM > PIM > CM. Among the other models, the TM exhibits the highest accuracy in fitting the subsidence in the mining area. Conversely, the CM has the lowest fitting accuracy. Compared to the conventional PIM, the TM shows a 13.8% improvement in fitting accuracy. As shown in Fig. 8, the subsidence impact range in the Jining mining area is significant. At the peripheral locations of the subsidence basin, the predicted values of the PIM model are lower than the measured values. On the other hand, at these locations, the predicted values of the other models are higher than those of the PIM. The ranking of fitting accuracy at the peripheral locations of the subsidence basin, from highest to lowest, is as follows: TM > LAM > LOM > PIM > CM. The TM demonstrates a 28.3% improvement in fitting accuracy compared to the traditional PIM. Therefore, using the TM to predict the boundary of surface subsidence in the mining area provides more precise results. Despite having the lowest fitting accuracy, the CM predicts higher values at the peripheral locations of the subsidence basin compared to other models. Hence, using the CM to predict the boundary of surface subsidence in the mining area ensures a safer approach.

According to Table 4, in the Heze mining area, all models have a relative error of less than 3% in fitting. Among the models, the TM exhibits the highest accuracy in fitting the subsidence in this mining area. Compared to the PIM, the TM shows a 22.2% improvement in the overall fitting accuracy of the entire subsidence basin. As shown in Fig. 9, the surface subsidence in the Heze mining area still follows a long-tail distribution pattern. At the peripheral locations of the subsidence basin, the TM demonstrates the highest fitting accuracy. Compared to the PIM, the TM shows a 63% improvement in fitting accuracy at these peripheral locations. Similarly, the CM predicts higher values at the peripheral locations of the subsidence basin compared to other models.

The Jining and Heze mining areas have thick alluvium, and subsidence in these areas typically exhibits a long-tail distribution pattern. The PIM, developed based on a normal distribution, does not accurately capture this long-tail distribution. Consequently, the accuracy of predicting surface subsidence using the PIM is relatively poor. It is crucial to accurately predict surface subsidence at the peripheral locations of the subsidence basin to determine the boundaries of mining-induced damage more precisely. After screening, the TM has been selected as the subsidence prediction model for both the Heze and Jining mining areas.

The experimental results indicate that, compared to the PIM, CPM can improve the accuracy of mining subsidence prediction.

Discussion

(1) Comparison of CPM with mechanics and numerical simulation methods.

Numerical simulation methods refer to using mechanics software developed based on finite element and discrete element methods to make predictions. It is evident that numerical simulation methods are essentially a form of mechanics methods. Relevant studies have shown that predictive models based on mechanics methods can effectively predict the movement patterns of overlying strata and surfaces (Qin et al. 2023). Additionally, mechanical methods can reveal the mechanisms behind surface subsidence. On the other hand, the CPM, which is based on influence function theory, is a mathematical method that does not consider the mechanical properties of rock mass. However, In China, it should be noted that the application of mechanics methods in predicting mining subsidence is not even as extensive as the use of PIM. There are several reasons for this:

Mechanics methods heavily rely on the existing data on geological conditions, subsurface formations, and soil properties in the study area. Taking a Jining mining area in Shandong Province, China as an example, Fig. 10 shows the stratigraphic information exposed by a specific borehole in this mining area. The number of rock layers in the stratigraphy of this mining area is more than 60. Engineers need to accurately test the mechanical strength and stiffness parameters of rock in each layer. Therefore, mechanics methods involve a significantly larger number of model parameters compared to PIM and CPM. This work is extremely challenging. Moreover, for some rocks with poor cementation properties, obtaining the core for some rocks is impossible, making it impossible to test their mechanical parameters. Even if the mechanical parameters of rocks are accurately measured, they may not be consistent with the rock mass

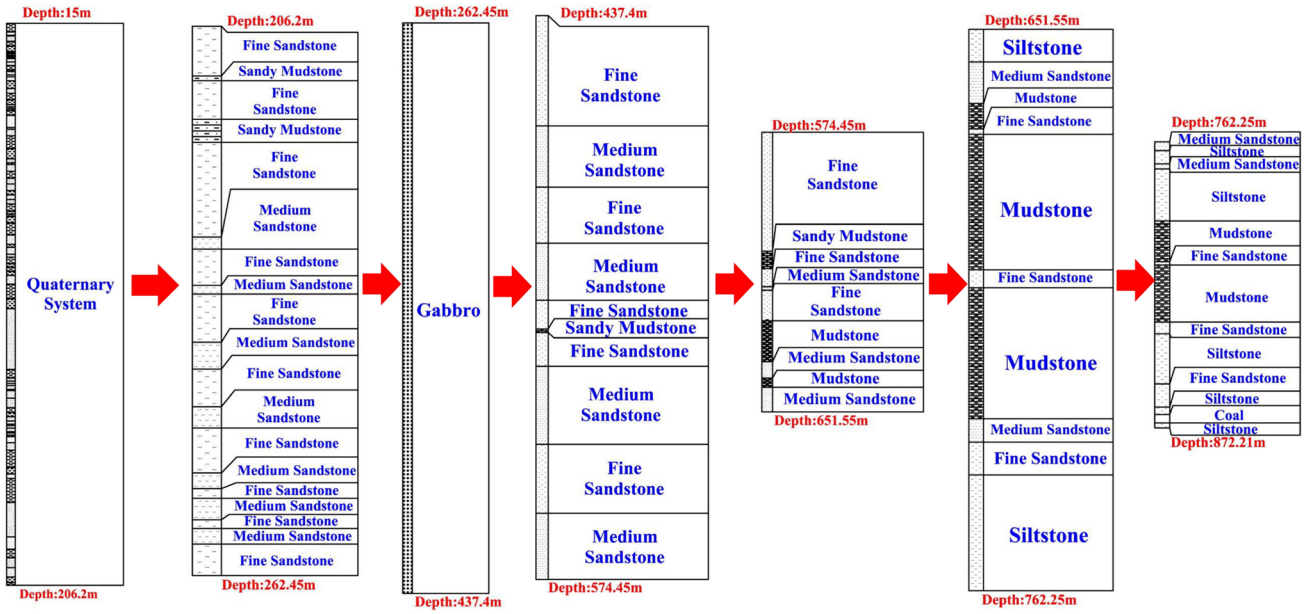

Fig. 10 Stratum information revealed by a borehole

parameters. In-situ testing experiments are required to measure the mechanical parameters of rock masses. There are still difficulties in accurately obtaining the mechanical parameters of rock mass in each layer. Additionally, the occurrence conditions of the overlying strata are extremely complex (Peng et al. 2015). Even two adjacent boreholes may have significant differences in the stratigraphic information they expose (Peng et al. 2015). Even rock masses with the same burial depth can have different lithology and thickness, so constructing a mechanical model based solely on the stratigraphic information from one borehole is inadequate. Additionally, the mechanical strength and stiffness parameters of different rock cores from the same rock layer, as measured in the laboratory, are inconsistent (Peng et al. 2015). As a result, conducting three-dimensional subsidence prediction using mechanics or numerical simulation methods requires extensive computational work. These limitations restrict the widespread adoption of this approach.

However, CPM has fewer parameters compared to mechanics methods. The predictive parameters of the CPM can be obtained by inverting surface movement observation data. Many mining areas in China have abundant surface movement observation data, which provides convenient conditions for obtaining predictive parameters of the CPM. Furthermore, as CPM is an extension of PIM, the parameters in both models have the same meaning, and their values are dependent on local geological and mining conditions. For instance, the subsidence factor q in the PIM and CPM is related to the mechanical strength and stiffness of rocks. The lower the strength of the overlying strata and the smaller the elastic modulus, the larger the subsidence factor. By adjusting the parameters in the model, it is possible to alter the shape of the predicted curve to achieve a closer fit with the measured subsidence curve.

Compared to mechanics methods, CPM is closer to an empirical approach as it abstracts the surface subsidence patterns into mathematical functions. Although this model does not consider the mechanical properties of rock masses, the fitting effect of this model on subsidence law is better than that of PIM commonly used in Chinese engineering. This viewpoint has been supported by experiments conducted in this study.

(2) Compared to other methods, such as PIM.

Many subsidence prediction equations, such as PIM or the subsidence prediction equation based on the Boltzmann function, are predictive models developed based on specific functions. However, these methods are not necessarily the optimal prediction methods in some mining areas. On the other hand, CPM does not have a specific expression and encourages engineers to screen appropriate probability distribution functions and incorporate them into CPM to establish prediction equations. This is a significant difference between CPM and other methods. This approach can further improve the accuracy of mining subsidence prediction and avoid limiting the improvement of prediction accuracy due to considering only one prediction method developed based on a specific function.

In the "Method Validation" section, based on the long-tailed characteristics of surface subsidence in the Heze and Jining mining areas, the TM model was constructed by selecting the T Location-Scale distribution and incorporating it into CPM. The TM is constructed based on

the T Location-Scale distribution and has a specific mathematical expression. Compared to the traditional PIM, the TM shows an improvement of 13.8% and 22.2% in fitting accuracy for subsidence in Jining and Heze, respectively. Compared to the PIM, the TM even shows a 63% improvement in fitting accuracy at peripheral locations of the subsidence basin. Additionally, TM exhibits higher prediction accuracy compared to LAM, LOM, and CM. The improved accuracy of subsidence prediction in these mining areas can be attributed to the CPM approach, which allows engineers to screen probability distribution functions instead of relying solely on PIM as the predictive method. In conclusion, the experimental results demonstrate that CPM contributes to improving the accuracy of subsidence prediction.

This study links prediction models for mining subsidence to probability theory. The research findings of this study indicate that the PDF can serve as the influence function (element subsidence function). CPM, fundamentally, is a mathematical expression composed of the CDF. Engineers only need to substitute the CDF of a given probability distribution into the CPM to develop a corresponding prediction model for mining subsidence. They do not have to ab-initio derive prediction equations for mining subsidence based on a specific function, reducing their workload. Therefore, this work also helps researchers understand the mathematical mechanisms underlying prediction models for mining subsidence.

Conclusions

(1) This study developed the CPM according to the influence function theory. CPM is an extension of PIM, sharing the same fundamental principles and application scope. CPM relates the probability distribution function to the subsidence prediction. CPM does not have a specific function expression. Instead, engineers are allowed to screen some unskewed continuous probability distribution functions to incorporate into this model and establish subsidence prediction equations. This approach can further improve the accuracy of mining subsidence prediction. This method provides engineers with more opportunities for selection. By not solely considering one prediction method developed based on a specific function, it avoids limiting the improvement of prediction accuracy.

(2) In the mining areas of Jining and Heze in China, surface subsidence exhibits a long-tail distribution characteristic. A T Location-Scale distribution was selected and incorporated into the CPM, and the TM model was constructed. Compared to the traditional PIM, the TM shows an improvement of 13.8% and 22.2% in fitting accuracy for subsidence in Jining and Heze, respectively. Additionally, the fitting precision of TM is higher than that of LAM, LOM, and CM when fitting mining subsidence with long-tailed distribution characteristics. This experiment confirms that CPM contributes to improving the accuracy of subsidence prediction.

Author contributions Hejian Yin: Conceptualization, Methodology, Software, Validation, Writing—Original Draft, Visualization. Guangli Guo: Conceptualization, Investigation, Resources, Writing—Review & Editing, Supervision, Funding acquisition. Huaizhan Li: Writing—Review & Editing. Tiening Wang: Writing—Review & Editing.

Funding This work was supported by the Joint Funds of the National Natural Science Foundation of China (Grant number U21A20109).

Data availability They are available from the corresponding author by request.

Declarations

Conflict of interests The authors declare that they have no conflict of interest.

References

Alaee NH, Mozafari A, Mirzaee M, Faghihi A, Tolouei K (2019) Fuzzy evaluation method for the identification of subsidence susceptibility in an underground mine (case study in Tabas coal mine of Iran). Nat Hazards 99(2):797–806. https://doi.org/10.1007/s11069-019-03774-2

Alam AKMB, Fujii Y, Eidee SJ, Boeut S, Rahim AB (2022) Prediction of mining-induced subsidence at Barapukuria longwall coal mine. Bangladesh Sci Rep 12(1):14800. https://doi.org/10.1038/s41598-022-19160-1

Chi SS, Wang L, Yu XX, Fang XJ, Jiang C (2021) Research on prediction model of mining subsidence in thick unconsolidated layer mining area. Ieee Access 9:23996–24010. https://doi.org/10.1109/access.2021.3056873

Deng KZ, Tan ZX, Jiang Y, Dai HY, Shi Y, Xu LJ (2014) Deformation monitoring and subsidence engineering, 1st edn. China University of Mining and Technology Press, Xuzhou, pp 187–219

Fang KT, Xu JL (2016) Statistical Distribution, 1st edn. Higher Education Press, Beijing, pp 193–204

Fernandez PR, Granda GR, Krzemien A, Cortes SG, Valverde GF (2020) Subsidence versus natural landslides when dealing with property damage liabilities in underground coal mines. Int J Rock Mech Min Sci 126:104175. https://doi.org/10.1016/j.ijrmms.2019.104175

Guo ZZ, Chai HB (2013) Coal mining subsidence studies, 1st edn. China Coal Industry Publishing House, Beijing, pp 25–26

Guo KK, Guo GL, Li HZ, Wang CY, Gong YQ (2020) Strata movement and surface subsidence prediction model of deep backfilling mining. ENERG SOURCE PART A 2020:1–15. https://doi.org/10.1080/15567036.2020.1838002

Gong YQ, Guo GL, Wang LP, Li HZ, Zhang GX, Fang Z (2022) A data-intensive numerical modeling method for large-scale rock strata and its application in mining subsidence prediction. Rock Mech Rock Eng 55(3):1687–1703. https://doi.org/10.1007/s00603-021-02745-z

Haciosmanoglu ME (2004) Development of a Subsidence Model for Çayirhan Coal Mine. Dissertation, Middle East Technical University

Jiang Y, Misa R, Tajdus K, Sroka A, Jiang Y (2020) A NEW PREDICTION MODEL OF SURFACE SUBSIDENCE WITH CAUCHY DISTRIBUTION IN THE COAL MINE OF THICK TOPSOIL CONDITION. Arch Min Sci. https://doi.org/10.24425/ams.2020.132712

Jirankova E, Waclawik P, Nemcik J (2020) Assessment of models to predict surface subsidence in the czech part of the upper silesian coal basin - case study. Acta Geodyn Geomater. https://doi.org/10.13168/agg.2020.0034

Jiang Q, Guo GL, Li HZ, Wei T, Yuan YF, Jiang CM (2022) Investigation of coordinated development of coal mining and pipeline protection under boundary effect of thick unconsolidated layer. Bull Eng Geol Environ. https://doi.org/10.1007/s10064-022-02636-9

Kratzsch H, Fleming RFS (1983) Mining Subsidence Engineering, 1st edn. Springer-Verlag, Berlin, New York, pp 194–227

Kwinta A, Gradka R (2020) Analysis of the damage influence range generated by underground mining. Int J Rock Mech Min Sci 128:104263. https://doi.org/10.1016/j.ijrmms.2020.104263

Kumar S, Kumar D, Donta PK, Amgoth T (2022) Land subsidence prediction using recurrent neural networks. Stoch Environ Res Risk Assess 36(2):373–388. https://doi.org/10.1007/s00477-021-02138-2

Li Y (2016) Robust Estimation Based on Laplace Distribution. Dissertation, Yangzhou University.

Liu SG, Li KX, Shi WP, Wang ZJ, Zhang HR, Li ZY (2022) Analysis of mining subsidence characteristics and deformation prediction considering size parameters and mechanical parameters. Geofluids. https://doi.org/10.1155/2022/5495509

Malinowska A, Hejmanowski R, Dai HY (2020) Ground movements modeling applying adjusted influence function. Int J Min Sci Technol 30(2):243–249. https://doi.org/10.1016/j.ijmst.2020.01.007

Ma JB, Yin DW, Jiang N, Wang S, Yao DH (2021) Application of a superposition model to evaluate surface asymmetric settlement in a mining area with thick bedrock and thin loose layer. J Clean Prod. https://doi.org/10.1016/j.jclepro.2021.128075

Peng SS, Zhou LHM, Y, et al (2015) Research on Ground Control in Shendong and Zhungeer Mining Areas, 1st edn. Science Press, Beijing, pp 268–269

Qin Z, Han X, Han JH (2023) A spatio-temporal predictive model for surface subsidence induced by mining in deep loose and thin bedrock strata. Mech Time-Depend Mater. https://doi.org/10.1007/s11043-023-09633-9

Salmi EF, Nazem M, Karakus M (2017) Numerical analysis of a large landslide induced by coal mining subsidence. Eng Geol 217:141–152. https://doi.org/10.1016/j.enggeo.2016.12.021

Saeidi A, Deck O, Seifaddini M, Heib MAL, Verdel T (2022) An improved methodology for applying the influence function for subsidence hazard prediction. Georisk 16(2):347–359. https://doi.org/10.1080/17499518.2021.1875247

Tajdus K, Misa R, Sroka A (2018) Analysis of the surface horizontal displacement changes due to longwall panel advance. Int J Rock Mech Min Sci 104:119–125. https://doi.org/10.1016/j.ijrmms.2018.02.005

Wang N, Wu K, Liu J, An SK (2013) Model for mining subsidence prediction based on Boltzmann function. J China Coal Soc. https://doi.org/10.13225/j.cnki.jccs.2013.08.018

Wang K, Li JZ, Jin ZP (2022) Influence of the primary key stratum on surface subsidence during longwall mining. Sustainability 14(22):1–15. https://doi.org/10.3390/su142215027

Wei T, Guo GL, Li HZ, Wang L, Jiang Q, Jiang CM (2023) A novel probability integral method segmental modified model for subsidence prediction applicable to thick loose layer mining areas. Environ Sci Pollut Res 30(18):52049–52061. https://doi.org/10.1007/s11356-023-26021-5

Xu C, Zhou KP, Xiong X, Gao F, Lu Y (2023) Prediction of mining induced subsidence by sparrow search algorithm with extreme gradient boosting and TOPSIS method. Acta Geotech 18(9):4993–5009. https://doi.org/10.1007/s11440-023-01830-7

Yang J, Luo Y (2021) Enhanced subsurface subsidence prediction model incorporating key strata theory. Mining Metall Explor 38(2):995–1008. https://doi.org/10.1007/s42461-021-00383-1

Yin HJ, Guo GL, Li HZ, Wang TN, Yuan YF (2022) Prediction method and research on characteristics of surface subsidence due to mining deeply buried Jurassic coal seams. Bull Eng Geol Environ. https://doi.org/10.1007/s10064-022-02946-y

Zhang JM, Yan YG, Dai HY, Xu LJ, Li JW, Xu RR (2022) Hyperbolic secant subsidence prediction model under thick loose layer mining area. Minerals. https://doi.org/10.3390/min12081023